HHS Public Access

Author manuscript

Mol Carcinog. Author manuscript; available in PMC 2019 January 01.

Published in final edited form as:

Mol Carcinog. 2018 January ; 57(1): 57–69. doi:10.1002/mc.22731.

Procyanidin B2 3,3″-di-O-gallate induces oxidative stress-mediated cell death in prostate cancer cells *via* inhibiting MAP kinase phosphatase activity and activating ERK1/2 and AMPK

Rahul Kumar[1], **Gagan Deep**[1,2], **Michael F. Wempe**[1,2], **Joseph Surek**[1], **Amit Kumar**[1], **Rajesh Agarwal**[1,2], and **Chapla Agarwal**[1,2,*]

[1]Department of Pharmaceutical Sciences, Skaggs School of Pharmacy, University of Colorado Denver, Aurora, CO, USA

[2]University of Colorado Cancer Center, University of Colorado Denver, Aurora, CO, USA

Abstract

Neoplastic cells exhibit higher oxidative stress compared to normal cells; however, antioxidants based clinical trials have mostly failed. Another attractive therapeutic approach is to further increase the oxidative stress in cancer cells leading to cell death. Herein, we show that Procyanidin B2 3,3″-di-O-gallate (B2G2), the most active constituent of grape seed extract, treatment causes cell death in human prostate cancer (PCa) cells (LNCaP and 22Rv1) via increasing the reactive oxygen species (ROS) generation. Mechanistically, B2G2 treatment decreased the mitochondrial electron transport chain complex III activity leading to enhanced mitochondrial superoxide generation and decreased ATP production in LNCaP cells. Additional molecular studies revealed that B2G2-induced cell death was mediated mainly through ROS-induced sustained activation of ERK1/2, which was due to inhibition of MAP kinase phosphatase (MKP) activity as over-expression of MKP3 in LNCaP cells conferred significant protection against B2G2-induced cell death. Along with ERK1/2, AMP-activated protein kinase α (AMPKα) was also activated by B2G2 treatment, and pre-treatment with AMPKα inhibitor compound C significantly reversed the cytotoxic effects of B2G2 in LNCaP cells. Furthermore, pre-treatment of MKP3 over-expressing LNCaP cells with compound C further reduced the B2G2-induced cell death, suggesting the involvement of AMPKα along with MKP3 and ERK1/2 in the biological effects of B2G2. Together, these results for the first time identified that oxidative stress and MKP3 inhibition play a critical role in B2G2-induced cell death in PCa cells through sustained activation of both ERK1/2 and AMPKα. These results offer a unique opportunity to control this deadly malignancy through B2G2 use.

Keywords

Prostate cancer; Procyanidin B2 3; 3″-di-O-gallate; Oxidative stress; Extracellular-signal-regulated kinase; Dual-specificity phosphoprotein phosphatase; AMP-activated kinase

*Corresponding Author: Chapla Agarwal, University of Colorado Denver, 12850 E. Montview Blvd, C238, Aurora, CO 80045. USA. Phone: (303) 724-4057, Fax: (303) 724-7266, Chapla.agarwal@ucdenver.edu.

INTRODUCTION

Prostate cancer (PCa) is the most common cancer in American men after the skin cancer. According to American Cancer Society estimates, in the year 2016, approximately 180,890 new cases of PCa will be diagnosed in the United States together with about 26,120 deaths; and mortality in American men due to PCa is second only to lung cancer [1]. PCa treatment includes hormonal ablation or androgen deprivation therapy (ADT), which is initially effective in almost all cases, but most of the patients eventually develop ADT resistance leading to castration-resistant PCa (CRPC) that is very aggressive [2]. Mechanistic studies suggest an association between oxidative stress and CRPC development, where PCa cells endogenously produce higher amounts of reactive oxygen species (ROS) promoting cell proliferation and genetic instability, a pre-requisite for cancer development and progression [3–6]. ROS, generated inside the cells as by-product of normal metabolism, could cause tissue injury and DNA damage but in normal cells, a dynamic balance is maintained between ROS level (pro-oxidant) and antioxidant proteins and enzymes. However, with the age this balance shifts toward pro-oxidant resulting in a chronic increase in ROS [7–9]. Based upon these observations, in the past, several studies have focused on using anti-oxidants for both preventive and therapeutic approaches in the management of PCa [10]. Consistent with this, different clinical trials have been conducted to assess the anti-cancer efficacy of several anti-oxidants. The most notable clinical trials are selenium and vitamin E cancer prevention trial known as SELECT and α-tocopherol and β-carotene prevention trial (referred as ATBC); however, these clinical trials failed to establish any relationship between overall PCa risk and dietary anti-oxidant consumption [11–14]. On the contrary, patient's follow-up in SELECT trial showed a significant increase in numbers of prostate cancer in men who took vitamin compared to men on placebo [15].

Along with the failure of several antioxidants, there is plethora of literature suggesting that elevated intracellular ROS level provides cancer cells an aggressive phenotype, however; ROS levels above a particular threshold could be deleterious to cancer cells [3,16]. Therefore, recent research efforts have also focused onto increase ROS production in cancer cells via compounds displaying pro-oxidant properties [17–20]. Importantly, compared to normal prostate epithelial cells, PCa cells generate higher amounts of ROS making them more prone to ROS-induced damages; enhanced ROS levels trigger pro-apoptotic signaling pathways as the anti-oxidant defense mechanisms are already compromised in these cancer cells [21–30]. In this regard, several dietary agents including grape seed extract (GSE) have been identified to cause apoptotic cell death in cancer cells by inducing oxidative stress [3,17–20,31–35]. GSE is a naturally occurring dietary agent with proven potential against various malignancies, including PCa [36]. Studies in our laboratory have identified procyanidin B2 3,3″-di-O-gallate (B2G2) as the most active constituent of GSE, and we have shown that B2G2 causes cell growth inhibition and apoptotic cell death in human PCa LNCaP, C4-2B, DU145 and PC-3 cells [37–40]. However, B2G2's mechanism(s) of action that causes cell death has not been elucidated, which is important in order to develop this promising molecule as an anti-cancer agent against PCa. Therefore, the focus of present study was to examine and establish the molecular mechanism underlying ROS generation and its role in B2G2-induced cell death in human PCa cells.

MATERIALS AND METHODS

Cell lines and reagents

Human PCa LNCaP (androgen dependent) and 22Rv1 (androgen independent) cells were purchased from ATCC (Manassas, VA) and maintained in RPMI1640 media supplemented with 100 U/ml penicillin, 100 μg/ml streptomycin and 10% FBS. PWR-1E cells (Human prostatic non-malignant epithelial cells) were purchased from ATCC and maintained in keratinocyte-SFM media (Thermo Fisher scientific). Antibodies for p-ERK1/2, ERK1/2, cleaved PARP, MKP2, MKP3, p-AMPKα, AMPKα and anti-rabbit peroxidase-conjugated secondary antibody were purchased from Cell Signaling (Beverly, MA). LC3 antibody was procured from Novus Biological (Littleton, CO). MKP1 and β-actin antibodies were obtained from Santa Cruz Biotechnology (Santa Cruz, CA). 2′,7′-Dichlorofluorescein diacetate (DCFDA), *N*-acetyl-L-cysteine (NAC), antimycin A, t-butyl hydrogen peroxide (H_2O_2) and JC-1 dye were purchased from Sigma-Aldrich Chemical Company (St Louis, MO). Mitosox red dye was acquired from Molecular Probes (Eugene, OR). PD98059 and compound C were bought from EMD Millipore (Billerica, MA). Complex I enzyme activity assay and MitoTox™ complex II + III OXPHOS activity assay kits were from Abcam (Cambridge, MA). B2G2 was synthesized according to our previously published methods [40]. B2G2 stock solution was prepared in DMSO and diluted in culture media to achieve the experimental concentrations. An equal amount of DMSO (vehicle) was present in each treatment, including control which did not exceed 0.1% (vol/vol).

Cell viability assay

LNCaP and 22Rv1 cells were seeded (5.0 x 10^4 cells/well) in 6-well culture plates. After 24 h, cells were treated with different concentrations of B2G2 (25–200 μM) for 24 h and 48 h. PWR-1E cells were seeded (5.0 x 10^4 cells/well) in 6-well culture plates in keratinocyte-SFM media with 10% FBS and treated with B2G2 (10–40 μM) for 24 h. At the end of each treatment time, cells were collected and total cell number and dead cell percentage were determined using a hemocytometer after trypan blue staining.

Cellular ROS measurement

For the estimation of ROS in LNCaP and 22Rv1 cells, 3.0 × 10^4 cells/well were plated in black 96-well plates with a clear bottom and, one day later, cellular monolayers were washed once with phenol red free RPMI1640 and subsequently stained (20 μM DCFDA; 45 min, 37°C). After washing the cells once with phenol red free RPMI1640, cells were treated with B2G2 (50 μM) and relative fluorescence intensity was measured at 1, 3, 6, 9, 12 and 24 h in a multi-well plate reader (Molecular Devices) using SoftMax software at an excitation and emission wavelengths of 485 and 535 nm, respectively. Background fluorescence was determined from wells containing cells without DCFDA and subtracted from respective fluorescence values.

Mitochondrial superoxide and mitochondrial membrane potential (MMP) measurements

Mitochondrial superoxide anions and mitochondrial membrane potential were measured by using live-cell permeative and mitochondrial selective MitoSOX red probe and JC-1 dye,

respectively as described previously [41,42]. Briefly, 3 X 10^4 cells/well were plated in black 96-well plates and after 36 hours cells were treated with 50 μM B2G2. After 6 hours of treatment with B2G2, cells were incubated in phenol red-free culture medium containing either 1 μM MitoSOX red probe or 5 μg/ml JC-1 dye at 37°C for 30 minutes. After incubation, cells were washed once with phenol-red free medium and fluorescence or absorbance was measured by using a multi-well plate reader (Spectra Max, Molecular Devices). MitoSOX red probe containing plate was read at an excitation and emission wavelengths of 510 and 580 nm, respectively. Absorbance of JC-1 dye labelled cells were read at both 590 nm and 530 nm wavelengths and mitochondrial membrane potential represented as ratio of absorbance values at 590 nm and 530 nm.

ATP measurement

For estimating the ATP content in LNCaP cells, cells were plated in 60 mm culture dishes, treated with B2G2 and ATP content measured using an ATP colorimetric kit as per the manufacturer's instructions (Biovision, Milpitas, CA).

Measurement of Mitochondrial complexes I and III activities

To measure mitochondrial complexes I and III activities, LNCaP cells were plated in 150 mm culture dishes and treated with B2G2 (50 μM) for 1, 3 and 6 h. At the end of each time point, mitochondria were isolated from the B2G2 treated LNCaP cells using a mitochondria isolation kit following the manufacturer's protocol (Thermo Scientific, Rockford, IL). The kinetics of complex I and III activities in 100 μg freshly isolated mitochondrial fractions were measured as described previously [19] and represented as a change in optical density per min (δ_{OD}/min).

To establish the direct effect of B2G2 on mitochondrial complex III activity, mitochondria were isolated from naïve LNCaP cells and 100 μg mitochondrial fractions were incubated with different concentrations of B2G2 (10–50 μM) and complex III activity was measured and represented as described above. Antimycin A (3.0 μM), a known inhibitor of mitochondrial complex III activity, was used as the positive control.

Immunoblotting

LNCaP cells were treated with different concentrations of B2G2 for the indicated time points and total cell lysates were prepared in non-denaturing lysis buffer [10 mM Tris–HCl, pH 7.4, 150 mM NaCl, 1% Triton X-100, 1.0 mM ethylene diamine tetra acetic acid, 1.0 mM ethylene glycol-bis (amino ethyl ether)-tetra acetic acid, 0.5% NP-40, 0.3 mM phenyl methyl sulfonyl fluoride, 0.2 mM sodium orthovanadate and 5.0 U/ml aprotinin]. Protein concentrations in the lysates were determined using DC Protein assay system (Bio Rad, Hercules, CA). For immunoblot analyses, 50–80 μg protein lysates were run on sodium dodecyl sulfate–polyacrylamide gels and blotted onto nitrocellulose membranes; they were then probed for the desired proteins using specific primary antibodies (dilution - 1:1000) followed by peroxidase-conjugated appropriate secondary antibody (dilution - 1: 2000) and subsequently visualized by enhanced chemiluminescence detection system (GE biosciences). Membranes were also stripped and re-probed again for other protein/s of interest, or β-actin antibody to ensure equal protein loading.

Generation of LNCaP-vector control and MKP3 overexpressing stable cell lines

LNCaP cells were transfected with lentiviral particles containing pLX304-MKP3 (Clone ID: ccsbBroad304_00468; GE Dharmacon, Lafayette, CO) or vector control pLX304 (a gift from David Root, Addgene plasmid # 25890) prepared by Functional genomics core, University of Colorado (Boulder, CO). Stable transduced cells were selected using blasticidin (8 μg/ml) in complete media for 3–4 weeks. The individual resistant clones were picked and grown separately and maintained in the same selection medium.

MAP kinase phosphatase activity assay

To assess the MAP kinase phosphatase activity, we first immobilize 1μg of purified phosphorylated-ERK2 protein (Catalogue # ab155812; Abcam, Cambridge, MA) on 20 μg Agarose conjugated-ERK2 antibody (Catalogue # sc-154 AC; Santa Cruz Biotechnology, Santa Cruz, CA) by incubating overnight in IP buffer (10 mM Tris, pH 7.5, 150 mM NaCl, 1.0 mM EDTA, 1.0 mM EGTA, 1% Triton X-100, 0.3 mM PMSF and 5.0 U/ml aprotinin). After that, agarose beads were pelleted down by centrifugation (3000 g, 2 min) and supernatant discarded and the unbound p-ERK2 removed from the pellet by washing twice with IP buffer. Finally the agarose beads were suspended in phosphatase activity buffer (50 mM Tris, pH 7.2, 150 mM NaCl, 1% NP-40, 0.3 mM PMSF and 5.0 U/ml aprotinin). Separately, LNCaP cells were treated with B2G2 with or without NAC for 6 h and protein lysates were prepared in phosphatase activity buffer. Protein lysates from LNCaP cells incubated with 1 mM H_2O_2 and from LNCaP-MKP3 cells served as negative and positive controls, respectively.

The immobilized p-ERK2 was separated into 6 equal parts and incubated (1 h, 37°C) with 20 μg protein lysates prepared above. Again, the agarose beads were pelleted by centrifugation (3000 g, 2 min) and washed twice with phosphatase activity buffer and re-suspended in 20 μl 2X SDS sample buffer, resolved on 8% SDS-PAGE and analyzed for p-ERK2 using anti-p-ERK1/2 antibody by immunoblotting as described above.

Statistics

All values are shown as mean ± standard error of mean (SEM). Differences in parameters between treatments were analyzed by ANOVA followed by Tukey post-hoc analysis and a P value of ≤ 0.05 was considered as statistically significant.

RESULTS

B2G2-induces cell death in human PCa cells via increasing oxidative stress

Earlier, we have reported the cytotoxic effect of B2G2 against human PCa cells LNCaP, 22Rv1, C4-2B, DU145 and PC3 cells [37–40]. Here, to ensure the effectiveness of new lot of synthetic prepared B2G2, we first confirmed the efficacy of B2G2 against two PCa cell lines LNCaP and 22Rv1 cells with the rationale that LNCaP cells are androgen dependent, whereas, 22Rv1 cells are androgen independent [43,44]. As shown in Figure 1A, B2G2 treatment (25 and 50 μM) resulted in 40–56% and 39–59% cell death at 24 h and 48 h, respectively in LNCaP cells; whereas in 22Rv1 cells, B2G2 treatment (50, 100 and 200 μM) caused 15–31% and 14–44% cell death at 24 h and 48 h, respectively (Figure 1B). Effect of

B2G2 on non-malignant human prostatic epithelial PWR-1E cells was also analyzed by trypan blue exclusion assay and as shown in Figure 1C, B2G2 treatment (10, 20, 30 and 40 μM) caused only 4–7.5% cell death at 24h indicating that B2G2 has negligible toxic effect on these cells.

Earlier reports have shown that GSE causes cell death in human head and neck and bladder carcinoma cells by oxidative stress induction [19,33], and since B2G2 is the major active constituent of GSE, we next measured whether B2G2 also induces ROS generation in human PCa LNCaP and 22Rv1 cells using DCFDA as a probe compound. Results showed a robust ROS generation by B2G2 treatment in both LNCaP and 22Rv1 cells (Figure 1D and 1E). As shown in Figure 1D, LNCaP cells showed higher ROS level following B2G2 treatment that peaked at 6 h and then gradually decreased to basal level by 24 h. Similarly, in 22Rv1 cells, B2G2 treatment resulted in increased ROS level that peaked at 9 h and then decreased to approximately basal level by 12 h (Figure 1E). As the effect of B2G2 was observed to be relatively robust in LNCaP cells compared to 22Rv1 cells in terms of both dead cells percentage and ROS generation, and also based upon the rationale that PCa is initially an androgen-dependent malignancy and mutation in AR is very common in PCa patients [43], we chose LNCaP cells which harbor T877A mutation for our further mechanistic studies.

NAC reverses B2G2-induced ROS generation and cell death in LNCaP cells

To demonstrate that B2G2-induced LNCaP cell death was due to ROS generation, next we pre-treated the LNCaP cells with an antioxidant NAC (10 mM) 15 min prior to B2G2 (50 μM) treatment. At the end (24 h), cells were observed under a phase-contrast microscope for gross morphological changes. As show in Figure 1F, B2G2 treatment caused a growth inhibition with significant increase in floating cells (generally, represent dead cells); while NAC pre-treatment resulted in a reversal of B2G2-caused changes in cell morphology and floaters (Figure 1F). Consistent with these morphological changes, NAC pre-treatment caused a 54% reduction in B2G2-induced ROS levels compared to the B2G2 alone treated group (Figure 1G). It was also observed that NAC pre-treatment significantly rescues LNCaP cells from B2G2-induced cell growth inhibition and cell death (Figure 1H). Overall, these results clearly suggest that B2G2 has pro-oxidant effects in human PCa cells and exerts its cytotoxic effects by generating ROS.

Effect of NAC on B2G2-induced mitochondrial superoxide production and MMP loss in LNCaP cells

Mitochondria and NADPH oxidase (NOX) system are considered as major sources of ROS generation [45–48]. Therefore, in order to identify the source of ROS following B2G2 treatments, we first assessed the effect of B2G2 on NOX activity in LNCaP cells and observed no change in its activity at 6 h (data not shown), a time-point when B2G2 treatment causes highest ROS generation as shown in Figure 1D. This ruled out NOX role in B2G2-induced ROS production in LNCaP cells. Next, we analyzed the effect of B2G2 treatment on mitochondrial superoxide generation using the mitochondria specific Mitosox red dye. As shown in Figure 2A, B2G2 treatment caused ~2 fold increase in mitochondrial superoxide levels at 6 h which was only partially affected by NAC pre-treatment. Since,

mitochondrial superoxide has been reported to depolarize MMP, we next assessed the effect of B2G2 treatment on MMP. As presented in Figure 2B, B2G2 treatment significantly reduced the MMP at 6 h that was also not affected by NAC pre-treatment. Furthermore, depolarization of MMP has been reported to cause a decrease in ATP production, and as shown in Figure 2C, B2G2 treatment (only at 50 μM) caused a significant decrease in ATP level in LNCaP cells at 6 h. Taken together, these results suggest that B2G2-induces oxidative stress via increasing ROS generation in mitochondria resulting in loss of MMP and inhibition in ATP generation, leading to cell death.

B2G2 inhibits mitochondrial complex III activity

The primary source of superoxide ion in mitochondria occurs via mitochondrial electron transport chain (ETC) complexes as electrons may leak from these complexes and react with oxygen to form superoxide ions [49]. Earlier studies suggest that mitochondrial OXPHOS complexes I and III are the major source of leaked electrons and thus superoxide generation [46,49]. Furthermore, our group recently reported that GSE induces mitochondrial superoxide generation in human head and neck cancer cells by inhibiting the activity of mitochondrial complex III [19]. Our results also showed that B2G2 treatment significantly inhibited complex III activity in LNCaP cells with no effect on complex I activity at all the tested time points (1, 3 and 6 h; Figure 2D and 2E), which was consistent with increased levels of ROS at 1 h and onwards (Figure 1D). In addition, in order to assess whether B2G2 inhibits complex III activity via direct interaction, we isolated mitochondria from naïve LNCaP cells and incubated with various concentrations of B2G2 and then assayed for complex III activity. As shown in Figure 2F, B2G2 directly inhibited complex III activity in a dose dependent manner. Overall, these results support the notion that inhibition of complex III activity by B2G2 could be the primary cause of pro-oxidant effects of B2G2 in LNCaP cells.

B2G2 activates ERK1/2 in LNCaP cells

It is well established that ROS-dependent sustained activation of ERK MAP kinases may be one of the probable reasons of its growth inhibitory effects [22,24,25,27,50,51]. Therefore, we analyzed the effect of B2G2 on ERK1/2 phosphorylation (Thr202/Tyr204), and as depicted in Figure 3A, significant activation of ERK1/2 was observed in LNCaP cells following B2G2 treatment (50 μM) at 3, 6, 9 and 12 h time points; whereas no ERK activation was observed at 30 and 40 μM doses. Next, we chose a 50 μM dose to observe the time-dependent activation of ERK1/2, and as presented in Figure 3B, ERK1/2 was activated by 3 h and remained activated up to 24 h following B2G2 exposure. To establish the role of ERK1/2 activation in B2G2-induced LNCaP cell death, we pre-treated cells with MEK inhibitor PD98059 (10, 25 and 50 μM) 15 min prior to B2G2 treatment. As displayed in Figure 3C and 3D, pre-treatment of PD98059 (50 μM) inhibited B2G2-induced ERK1/2 activation and PARP cleavage (a marker of apoptotic cell death) as well as significantly compromised the B2G2-induced cell growth inhibition and cell death in LNCaP cells. Moreover, we also observed that NAC pre-treatment inhibited B2G2-induced ERK1/2 activation at 6 h and 9 h (Figure 3E) as well as PARP cleavage (Figure 3F); these experimental observation were consistent with our above mentioned observation where NAC pre-treatment inhibited the B2G2-induced LNCaP cell death (Fig. 1H). These results

strongly suggest that B2G2-induced sustained ERK1/2 activation could be a key molecular event in its cytotoxic effects in LNCaP cells.

B2G2 strongly inhibits MAP kinase phosphatase 3 activity in LNCaP cells

As mentioned in the introduction that ROS-induced inhibition of MKPs may leads to sustained activation of ERK, we next analyzed MKP1, 2 and 3 protein levels in LNCaP cells following B2G2 treatment at 1, 3, 6 and 24 h. As shown in Figure 4A, B2G2 treatment only decreased the MKP3 expression at 3, 6 and 24 h, but not MKP1 and 2. Earlier reports suggest that MKPs contain a protein tyrosine phosphatase (PTP) domain with cysteine residues which could be oxidized by ROS resulting in MKP inactivation [52,53]. Therefore, we next assessed the effect of B2G2 on MKP activity using purified p-ERK2 as a substrate. As presented in Figure 4B, de-phosphorylation of p-ERK2 was inhibited following B2G2 treatment suggesting an inhibition of MKP activity. Importantly, NAC pre-treatment restored the MPK activity inhibited by B2G2 treatment (Figure 4B). These results clearly suggested that B2G2-induced ROS generation activates ERK by inhibiting MKPs activity.

As only MKP3 was observed to be down regulated following B2G2 treatment, we over-expressed MKP3 in LNCaP cells (Figure 4C) and then assessed its role. There was no ERK1/2 phosphorylation observed in MKP3 over-expressing LNCaP (LNCaP-MKP3) cells following B2G2 treatment; in contrast, B2G2 treatment decreased the MKP3 level and increased the ERK1/2 phosphorylation in empty vector transduced LNCaP (LNCaP-VC) cells (Figure 4D). These results confirmed that inhibition in MKP3 activity is responsible for B2G2-induced sustained ERK1/2 activation. Furthermore, the effect of B2G2 on cell death in LNCaP-VC and LNCaP-MKP3 cells were also analyzed by trypan blue staining assay. Results showed that B2G2 treatment in LNCaP-VC cells caused significant cell growth inhibition (by 65%) and increased the percentage dead cells (~4.5 folds) compared to vehicle treated LNCaP-VC cells (Figure 4E). However, the cytotoxic effects of B2G2 were significantly compromised in LNCaP-MKP3 cells with only 30% cell growth inhibition and ~3.4 fold increase in percentage dead cell compared to vehicle treated LNCaP-MKP3 cells (Figure 4E). Furthermore, B2G2-induced PARP cleavage was relatively compromised in LNCaP-MKP3 cells compared to LNCaP-VC cells (Figure 4F). Importantly, results with LNCaP-MKP3 cells were comparable with PD98059 pre-treated LNCaP cells; the percentage of dead cells in both conditions showed ~30% dead cells following B2G2 treatment. Taken together, these results strongly suggest the role of ERK1/2 activation in B2G2-induced cell death in LNCaP cells.

B2G2 activates cellular energy sensor AMPK in LNCaP cells

As presented in above, pre-treatment of LNCaP cells with MEK inhibitor PD98059 significantly inhibited B2G2-induced cell death, and the cytotoxic effects of B2G2 were also compromised in LNCaP-MKP3 cells. In both conditions the reversal in B2G2-induced cell death was found to be approximately 50% when compared to control; which indicates the involvement of other pathways in B2G2-induced cytotoxicity. Interestingly, as mentioned above, B2G2 treatment decreases cellular ATP level, indicating energy stress in LNCaP cells (Figure 2C). Therefore, we further assessed the effect of B2G2 on AMPK activation, a biomarker for cellular energy status. As shown in Figure 5A, AMPKα phosphorylation

(Thr172) was enhanced in LNCaP cells at 6, 9 and 24 h following B2G2 treatment; and NAC pre-treatment inhibited the AMPKα phosphorylation. In addition to analyzing AMPKα phosphorylation levels, we also analyzed LC3B-II/LC3B-1 ratio in LNCaP cells following B2G2 treatment with the rationale that higher LC3B cleavage is one of the hallmarks of autophagy and LC3B-II/LC3B-1 ratio was found to be increased in B2G2 treated LNCaP cells at 6 and 9 h (Figure 5B). It has been reported that ERK1/2 could activate AMPKα phosphorylation in mouse hypothalamic GT1-7 cells [54]]. Therefore, we assessed the effect of MEK inhibitor PD98059 on AMPKα phosphorylation. As shown in Figure 5C, pre-treatment of PD98059 had no significant effect on B2G2-induced AMPKα phosphorylation. These results supported the notion that ERK1/2 is not involved in AMPKα activation. Next, to assess the involvement of AMPKα in B2G2-induced growth inhibition and death in LNCaP cells, we pre-treated LNCaP cells with compound C, a specific pharmacological AMPK inhibitor. As presented in Figure 5D, compound C significantly reversed the B2G2-induced cell growth inhibition and cell death; and as shown above in Figure 3F, compound C completely reversed the B2G2-induced PARP cleavage. These results suggested that along with ERK activation, AMPK activation is also an important event in B2G2-induced cytotoxicity in LNCaP cells. To further confirm the involvement of AMPK in B2G2-induced cell death, we treated LNCaP-MKP3 cells with compound C 15 min prior to B2G2 treatment and then analyzed the status of AMPKα phosphorylation and PARP cleavage, and determined the total cell number and percentage cell death. As shown in Figure 5E, pre-treatment with compound C inhibited AMPKα phosphorylation and PARP cleavage in both LNCaP-VC and LNCaP-MKP3 cells; however, lesser AMPKα phosphorylation was observed in LNCaP-MKP3 cells compared to LNCaP-VC cells. Similarly, compound C significantly reversed the cell growth inhibition and percentage cell death in LNCaP-VC cells; however, B2G2 cytotoxic effects were compromised in LNCaP-MPK3 cells. Furthermore, compound C pre-treatment of LNCaP-MKP3 cells caused only 18% cell death, which was not significant when compared to control cells (Figure 5F). This result is of importance because it provides first concrete evidence that both ERK1/2 and AMPKα activation by B2G2 are required for its action against human PCa LNCaP cells.

Discussion

PCa is a major health burden worldwide. In this regard, chemoprevention using non-toxic natural compounds has become an attractive approach and has emerged as a promising and cost-effective approach to manage PCa. One such natural compound is B2G2, the most active constituent of GSE, which is a complex mixture of various Procyanidin and already marketed in the United States as a dietary supplement [37]. The cytotoxic potential of B2G2 against PCa cells has already been shown by us in our previous publications and in the present study we provide first evidence that B2G2 causes cell death in PCa cells by: i) induction of oxidative stress by inhibiting mitochondrial electron transport complex III activity; ii) oxidative stress which leads to sustained activation of ERK1/2 by inactivating MAP kinase phosphatases activity; and iii) through activation of cellular energy sensor AMPKα.

Our study shows that B2G2 displays strong pro-oxidant properties by generating appreciable amounts of intracellular ROS. The major sources of intracellular ROS include NOX system

and mitochondrial electron transport chain (ETC). Since NOX activity was not affected by B2G2 treatment, it seems B2G2-mediated increased ROS is primarily through targeting the mitochondrial ETC. The primary function of the mitochondrial ETC is ATP synthesis by creating an electrochemical proton gradient between inter-membrane space and mitochondrial matrix; then use the energy derived from redox reactions by transferring electrons from electron donors to electron acceptors [46,49]. During these redox reactions, electrons may leak from the respiratory chain and react with oxygen to form superoxide ions ($O_2^{\cdot -}$); complex I and III have been previously identified as the major sites of this electron leakage [46,49]. Earlier studies with antimycin A (a specific complex III inhibitor), GSE, benzyl isothiocyanate (BITC) and phenyl isothiocyanate (PITC) showed that inhibition of complex III leads to intracellular ROS generation in various cancer cells [17–19,55]. Likewise, in the present study, B2G2 was found to significantly inhibit complex III activity with no effect on complex I activity; and thus complex III is the major source of B2G2-induced mitochondrial superoxide and H_2O_2 generation. Furthermore, mitochondrial superoxide generation leads to depolarization of MMP, and together with deficient complex III activity, results in decreased ATP generation and energy stress in the cells as observed in the present study.

Physiological levels of ROS are reported to affect cellular signaling pathways and thereby regulate diverse cellular processes. On the other hand, excessive amounts of ROS ultimately contribute to cell death [3,4,29,30]. Our results clearly showed that B2G2-induces cell death in PCa cells via ROS mediated processes as NAC pre-treatment reversed the B2G2's cytotoxic effects. ROS primarily causes cell death by damaging cellular macromolecules like DNA, proteins and lipids; however, recent research showed that ROS-induced cell death may also be mediated by ERK1/2 activation [21,22,28]. ERK1/2 activation is primarily associated with survival and cell proliferation. Whereas, it has been shown that sustained ERK activation also contributed towards cell death, especially the DNA-damaging agents like cisplatin, etoposide, UV-irradiation and ROS are reported to cause apoptotic cell death by activating ERK1/2 [26,28]. This differential effect of ERK1/2 on cellular responses has been dependent upon the duration of its activation with a rapid and transient activation appears to linked with cell proliferation, whereas a sustained activation seems to relate with apoptotic cell death [56]. In the present study, we observed that B2G2-mediated ERK1/2 activation was sustained even after 24 h. ERK1/2 role in B2G2-induced cell death was further supported by the finding that MEK inhibitor PD98059 pre-treatment reversed the B2G2-induced cell death.

ROS causes sustained ERK1/2 activation and one of the mechanisms is through inactivation and degradation of protein phosphatases [53,57,58]. Protein phosphatases for MAP kinases are dual specificity phosphatases also called MAPK phosphatases (MKPs) and negatively regulate the MAPK signaling by dephosphorylating both threonine/tyrosine residues within the activation loop of MAPK [58]. Among MKPs, MKP1, 2, and 3 are reported to regulate the ERK1/2 activation negatively [59]. Our results showed that B2G2 down regulates the expression of MKP3 but not MKP1 & MKP2 along with its ability to inhibit overall MKP activity. These MKPs contain cysteine residues in their active domain which are redox sensitive and ROS can oxidize these residues leading to inhibition of their activity [53,58]; our results also illustrated that NAC pre-treatment restores B2G2-inhibited MKP activity.

Furthermore, we also show that B2G2 effects are compromised in MKP3 overexpressing LNCaP cells; thereby, confirming the MKP3 role in B2G2-induced ERK1/2 activation and cell death.

One of the major observations from the current study is that neither pre-treatment with MEK inhibitor PD98059 nor overexpression of MKP3 completely reversed the B2G2-induced cell death in LNCaP cells. In this regard, we also observed that B2G2 treatment decreased the ATP level which could lead to AMPKα activation, thereby activating an additional pathway contributing towards B2G2-induced cell death and working in tandem with ERK1/2 activation. Our results illustrated that B2G2 induces phosphorylation of the α-catalytic subunit of AMPK which may be due to both energetic stress and oxidative stress. AMPK is a highly conserved cellular energy sensor and primarily activated by an increased AMP/ATP ratio due to lowered ATP levels i.e. energetic stress. In addition, another mode of AMPK activation is ROS-mediated S-glutathionylation of cysteine residues within the α-catalytic subunit of AMPK i.e. oxidative stress [60]. The involvement of ROS in B2G2-induced AMPKα activation was confirmed by the observation that pre-treatment with NAC inhibits AMPKα phosphorylation. In addition, pre-treatment of LNCaP cells with AMPK inhibitor compound C was found to reverse B2G2-induced growth inhibition and cell death, which further confirmed the role of AMPK in the observed B2G2-induced biological effects. Previous studies also reported the activation of AMPK in response to energetic and oxidative stress leading to apoptotic cell death in cancer cells and is considered as an important target for cancer therapy [60]. Similarly, Kaur *et al.* have shown that AMPKα inhibition reversed bitter melon juice-induced caspase 3 activation in human pancreatic BxPC-3 cells [61]. Lastly, AMPK inhibition in MKP3 overexpressing LNCaP cells almost completely reversed the B2G2-induced cell death, further supporting the role of ROS-mediated AMPK and ERK1/2 activation as a probable mechanism for B2G2 efficacy against PCa cells.

In conclusion, we have demonstrated that B2G2 possesses strong pro-oxidant property and targets mitochondrial electron transport complex III leading to ROS generation causing oxidative and energetic stress in human prostate LNCaP cells. Molecular studies revealed that B2G2 inhibits MKP3 activity resulting in sustained activation of ERK1/2 and AMPKα; and this modulation in redox signaling underlies B2G2-induced biological effects in LNCaP cells (summarized in Figure 6). These promising findings need to be further validated in relevant in vivo PCa models for potential translational application.

Acknowledgments

Grant Support: This work was supported by NCI R01 grants CA91883 and CA195708. The research utilized services of the Medicinal Chemistry Core Facility (MCCF) to synthesize the B2G2. The Medicinal Chemistry Core facility receives funding via CCTSI, an institute at the University of Colorado Denver supported in part by NIH/NCATS Colorado CTSI Grant Number UL1TR001082.

List of Abbreviations

ADT	Androgen deprivation therapy
AMPKα	Adenosine monophosphate-activated protein kinase alpha

ANOVA	Analysis of variance
ATP	Adenosine triphosphate
B2G2	Procyanidin B2 3,3″-di-O-gallate
CRPC	Castration-resistant prostate cancer
DCFDA	2′,7′-Dichlorofluorescein diacetate
ERK1/2	Extracellular signal-regulated kinase 1/2
GSE	Grape seed extract
MKP	MAP kinase phosphatase
NAC	*N*-acetyl-L-cysteine
PCa	Prostate cancer
ROS	Reactive oxygen species
SEM	Standard error of mean

References

1. Siegel RL, Miller KD, Jemal A. Cancer statistics, 2016. CA Cancer J Clin. 2016; 66:7–30. [PubMed: 26742998]
2. Sharifi N, Gulley JL, Dahut WL. An update on androgen deprivation therapy for prostate cancer. Endocrine-related cancer. 2010; 17:R305–315. [PubMed: 20861285]
3. Acharya A, Das I, Chandhok D, Saha T. Redox regulation in cancer: a double-edged sword with therapeutic potential. Oxid Med Cell Longev. 2010; 3:23–34. [PubMed: 20716925]
4. Kang SW, Lee S, Lee EK. ROS and energy metabolism in cancer cells: alliance for fast growth. Archives of pharmacal research. 2015
5. Khandrika L, Kumar B, Koul S, Maroni P, Koul HK. Oxidative stress in prostate cancer. Cancer Lett. 2009; 282:125–136. [PubMed: 19185987]
6. Minelli A, Bellezza I, Conte C, Culig Z. Oxidative stress-related aging: A role for prostate cancer? Biochimica et biophysica acta. 2009; 1795:83–91. [PubMed: 19121370]
7. Battisti V, Maders LD, Bagatini MD, et al. Oxidative stress and antioxidant status in prostate cancer patients: relation to Gleason score, treatment and bone metastasis. Biomed Pharmacother. 2011; 65:516–524. [PubMed: 21993000]
8. Shiota M, Yokomizo A, Naito S. Oxidative stress and androgen receptor signaling in the development and progression of castration-resistant prostate cancer. Free radical biology & medicine. 2011; 51:1320–1328. [PubMed: 21820046]
9. Geybels MS, van den Brandt PA, van Schooten FJ, Verhage BA. Oxidative stress-related genetic variants, pro- and antioxidant intake and status, and advanced prostate cancer risk. Cancer epidemiology, biomarkers & prevention : a publication of the American Association for Cancer Research, cosponsored by the American Society of Preventive Oncology. 2015; 24:178–186.
10. Ting H, Deep G, Agarwal C, Agarwal R. The strategies to control prostate cancer by chemoprevention approaches. Mutation research Fundamental and molecular mechanisms of mutagenesis. 2014; 760:1–15. [PubMed: 24389535]
11. Gaziano JM, Glynn RJ, Christen WG, et al. Vitamins E and C in the prevention of prostate and total cancer in men: the Physicians' Health Study II randomized controlled trial. Jama. 2009; 301:52–62. [PubMed: 19066368]

12. Lonn E, Bosch J, Yusuf S, et al. Effects of long-term vitamin E supplementation on cardiovascular events and cancer: a randomized controlled trial. Jama. 2005; 293:1338–1347. [PubMed: 15769967]
13. Kirsh VA, Hayes RB, Mayne ST, et al. Supplemental and dietary vitamin E, beta-carotene, and vitamin C intakes and prostate cancer risk. Journal of the National Cancer Institute. 2006; 98:245–254. [PubMed: 16478743]
14. Heinonen OP, Albanes D, Virtamo J, et al. Prostate cancer and supplementation with alpha-tocopherol and beta-carotene: incidence and mortality in a controlled trial. Journal of the National Cancer Institute. 1998; 90:440–446. [PubMed: 9521168]
15. Klein EA, Thompson IM Jr, Tangen CM, et al. Vitamin E and the risk of prostate cancer: the Selenium and Vitamin E Cancer Prevention Trial (SELECT). Jama. 2011; 306:1549–1556. [PubMed: 21990298]
16. Trachootham D, Alexandre J, Huang P. Targeting cancer cells by ROS-mediated mechanisms: a radical therapeutic approach? Nature reviews Drug discovery. 2009; 8:579–591. [PubMed: 19478820]
17. Xiao D, Powolny AA, Singh SV. Benzyl isothiocyanate targets mitochondrial respiratory chain to trigger reactive oxygen species-dependent apoptosis in human breast cancer cells. The Journal of biological chemistry. 2008; 283:30151–30163. [PubMed: 18768478]
18. Xiao D, Powolny AA, Moura MB, et al. Phenethyl isothiocyanate inhibits oxidative phosphorylation to trigger reactive oxygen species-mediated death of human prostate cancer cells. J Biol Chem. 2010; 285:26558–26569. [PubMed: 20571029]
19. Shrotriya S, Deep G, Lopert P, Patel M, Agarwal R, Agarwal C. Grape seed extract targets mitochondrial electron transport chain complex III and induces oxidative and metabolic stress leading to cytoprotective autophagy and apoptotic death in human head and neck cancer cells. Mol Carcinog. 2014
20. Gorrini C, Harris IS, Mak TW. Modulation of oxidative stress as an anticancer strategy. Nat Rev Drug Discov. 2013; 12:931–947. [PubMed: 24287781]
21. Zhuang S, Yan Y, Daubert RA, Han J, Schnellmann RG. ERK promotes hydrogen peroxide-induced apoptosis through caspase-3 activation and inhibition of Akt in renal epithelial cells. American journal of physiology Renal physiology. 2007; 292:F440–447. [PubMed: 16885155]
22. Zhuang S, Schnellmann RG. A death-promoting role for extracellular signal-regulated kinase. The Journal of pharmacology and experimental therapeutics. 2006; 319:991–997. [PubMed: 16801453]
23. Stanciu M, Wang Y, Kentor R, et al. Persistent activation of ERK contributes to glutamate-induced oxidative toxicity in a neuronal cell line and primary cortical neuron cultures. The Journal of biological chemistry. 2000; 275:12200–12206. [PubMed: 10766856]
24. Torres M. Mitogen-activated protein kinase pathways in redox signaling. Frontiers in bioscience : a journal and virtual library. 2003; 8:d369–391. [PubMed: 12456373]
25. Tai P, Ascoli M. Reactive oxygen species (ROS) play a critical role in the cAMP-induced activation of Ras and the phosphorylation of ERK1/2 in Leydig cells. Molecular endocrinology. 2011; 25:885–893. [PubMed: 21330403]
26. Mebratu Y, Tesfaigzi Y. How ERK1/2 activation controls cell proliferation and cell death: Is subcellular localization the answer? Cell cycle. 2009; 8:1168–1175. [PubMed: 19282669]
27. Martin P, Pognonec P. ERK and cell death: cadmium toxicity, sustained ERK activation and cell death. The FEBS journal. 2010; 277:39–46. [PubMed: 19843171]
28. Lee YJ, Cho HN, Soh JW, et al. Oxidative stress-induced apoptosis is mediated by ERK1/2 phosphorylation. Experimental cell research. 2003; 291:251–266. [PubMed: 14597424]
29. Sabharwal SS, Schumacker PT. Mitochondrial ROS in cancer: initiators, amplifiers or an Achilles' heel? Nat Rev Cancer. 2014; 14:709–721. [PubMed: 25342630]
30. Ivanova D, Bakalova R, Lazarova D, Gadjeva V, Zhelev Z. The impact of reactive oxygen species on anticancer therapeutic strategies. Advances in clinical and experimental medicine : official organ Wroclaw Medical University. 2013; 22:899–908. [PubMed: 24431321]
31. Das TP, Suman S, Damodaran C. Induction of reactive oxygen species generation inhibits epithelial-mesenchymal transition and promotes growth arrest in prostate cancer cells. Molecular carcinogenesis. 2014; 53:537–547. [PubMed: 23475579]

32. Kim KY, Yu SN, Lee SY, et al. Salinomycin-induced apoptosis of human prostate cancer cells due to accumulated reactive oxygen species and mitochondrial membrane depolarization. Biochemical and biophysical research communications. 2011; 413:80–86. [PubMed: 21871443]
33. Raina K, Tyagi A, Kumar D, Agarwal R, Agarwal C. Role of oxidative stress in cytotoxicity of grape seed extract in human bladder cancer cells. Food and chemical toxicology : an international journal published for the British Industrial Biological Research Association. 2013; 61:187–195. [PubMed: 23831192]
34. Lee W, Kim KY, Yu SN, et al. Pipernonaline from Piper longum Linn. induces ROS-mediated apoptosis in human prostate cancer PC-3 cells. Biochemical and biophysical research communications. 2013; 430:406–412. [PubMed: 23159637]
35. Ketola K, Vainio P, Fey V, Kallioniemi O, Iljin K. Monensin is a potent inducer of oxidative stress and inhibitor of androgen signaling leading to apoptosis in prostate cancer cells. Molecular cancer therapeutics. 2010; 9:3175–3185. [PubMed: 21159605]
36. Kaur M, Agarwal C, Agarwal R. Anticancer and cancer chemopreventive potential of grape seed extract and other grape-based products. J Nutr. 2009; 139:1806S–1812S. [PubMed: 19640973]
37. Agarwal C, Veluri R, Kaur M, Chou SC, Thompson JA, Agarwal R. Fractionation of high molecular weight tannins in grape seed extract and identification of procyanidin B2–3,3′-di-O-gallate as a major active constituent causing growth inhibition and apoptotic death of DU145 human prostate carcinoma cells. Carcinogenesis. 2007; 28:1478–1484. [PubMed: 17331955]
38. Chou SC, Kaur M, Thompson JA, Agarwal R, Agarwal C. Influence of gallate esterification on the activity of procyanidin B2 in androgen-dependent human prostate carcinoma LNCaP cells. Pharmaceutical research. 2010; 27:619–627. [PubMed: 20162340]
39. Shrestha SP, Thompson JA, Wempe MF, Gu M, Agarwal R, Agarwal C. Glucuronidation and methylation of procyanidin dimers b2 and 3,3″-di-o-galloyl-b2 and corresponding monomers epicatechin and 3-o-galloyl-epicatechin in mouse liver. Pharmaceutical research. 2012; 29:856–865. [PubMed: 22068277]
40. Tyagi A, Raina K, Shrestha SP, et al. Procyanidin B2 3,3(″)-di-O-gallate, a biologically active constituent of grape seed extract, induces apoptosis in human prostate cancer cells via targeting NF-kappaB, Stat3, and AP1 transcription factors. Nutrition and cancer. 2014; 66:736–746. [PubMed: 24191894]
41. Dalla Pozza E, Donadelli M, Costanzo C, et al. Gemcitabine response in pancreatic adenocarcinoma cells is synergistically enhanced by dithiocarbamate derivatives. Free radical biology & medicine. 2011; 50:926–933. [PubMed: 21236335]
42. Mishra V, Saxena DK, Das M. Effect of argemone oil and argemone alkaloid, sanguinarine on Sertoli-germ cell coculture. Toxicology letters. 2009; 186:104–110. [PubMed: 19429230]
43. Sun C, Shi Y, Xu LL, et al. Androgen receptor mutation (T877A) promotes prostate cancer cell growth and cell survival. Oncogene. 2006; 25:3905–3913. [PubMed: 16636679]
44. Li Y, Chan SC, Brand LJ, Hwang TH, Silverstein KA, Dehm SM. Androgen receptor splice variants mediate enzalutamide resistance in castration-resistant prostate cancer cell lines. Cancer Res. 2013; 73:483–489. [PubMed: 23117885]
45. Bleier L, Drose S. Superoxide generation by complex III: from mechanistic rationales to functional consequences. Biochimica et biophysica acta. 2013; 1827:1320–1331. [PubMed: 23269318]
46. Drose S, Brandt U. Molecular mechanisms of superoxide production by the mitochondrial respiratory chain. Advances in experimental medicine and biology. 2012; 748:145–169. [PubMed: 22729857]
47. Lambeth JD, Neish AS. Nox enzymes and new thinking on reactive oxygen: a double-edged sword revisited. Annual review of pathology. 2014; 9:119–145.
48. Stanley A, Thompson K, Hynes A, Brakebusch C, Quondamatteo F. NADPH oxidase complex-derived reactive oxygen species, the actin cytoskeleton, and Rho GTPases in cell migration. Antioxidants & redox signaling. 2014; 20:2026–2042. [PubMed: 24251358]
49. Brand MD, Affourtit C, Esteves TC, et al. Mitochondrial superoxide: production, biological effects, and activation of uncoupling proteins. Free radical biology & medicine. 2004; 37:755–767. [PubMed: 15304252]

50. Deschenes-Simard X, Kottakis F, Meloche S, Ferbeyre G. ERKs in cancer: friends or foes? Cancer research. 2014; 74:412–419. [PubMed: 24408923]
51. Cagnol S, Chambard JC. ERK and cell death: mechanisms of ERK-induced cell death--apoptosis, autophagy and senescence. The FEBS journal. 2010; 277:2–21. [PubMed: 19843174]
52. Miki H, Funato Y. Regulation of intracellular signalling through cysteine oxidation by reactive oxygen species. Journal of biochemistry. 2012; 151:255–261. [PubMed: 22287686]
53. Keyse SM. Dual-specificity MAP kinase phosphatases (MKPs) and cancer. Cancer metastasis reviews. 2008; 27:253–261. [PubMed: 18330678]
54. Damm E, Buech TR, Gudermann T, Breit A. Melanocortin-induced PKA activation inhibits AMPK activity via ERK-1/2 and LKB-1 in hypothalamic GT1–7 cells. Molecular endocrinology. 2012; 26:643–654. [PubMed: 22361823]
55. Turrens JF, Alexandre A, Lehninger AL. Ubisemiquinone is the electron donor for superoxide formation by complex III of heart mitochondria. Archives of biochemistry and biophysics. 1985; 237:408–414. [PubMed: 2983613]
56. Seifried HE, Anderson DE, Fisher EI, Milner JA. A review of the interaction among dietary antioxidants and reactive oxygen species. The Journal of nutritional biochemistry. 2007; 18:567–579. [PubMed: 17360173]
57. Haagenson KK, Wu GS. Mitogen activated protein kinase phosphatases and cancer. Cancer biology & therapy. 2010; 9:337–340. [PubMed: 20139719]
58. Patterson KI, Brummer T, O'Brien PM, Daly RJ. Dual-specificity phosphatases: critical regulators with diverse cellular targets. The Biochemical journal. 2009; 418:475–489. [PubMed: 19228121]
59. Kim HS, Song MC, Kwak IH, Park TJ, Lim IK. Constitutive induction of p-Erk1/2 accompanied by reduced activities of protein phosphatases 1 and 2A and MKP3 due to reactive oxygen species during cellular senescence. The Journal of biological chemistry. 2003; 278:37497–37510. [PubMed: 12840032]
60. Jeon SM, Hay N. The double-edged sword of AMPK signaling in cancer and its therapeutic implications. Archives of pharmacal research. 2015
61. Kaur M, Deep G, Jain AK, et al. Bitter melon juice activates cellular energy sensor AMP-activated protein kinase causing apoptotic death of human pancreatic carcinoma cells. Carcinogenesis. 2013; 34:1585–1592. [PubMed: 23475945]

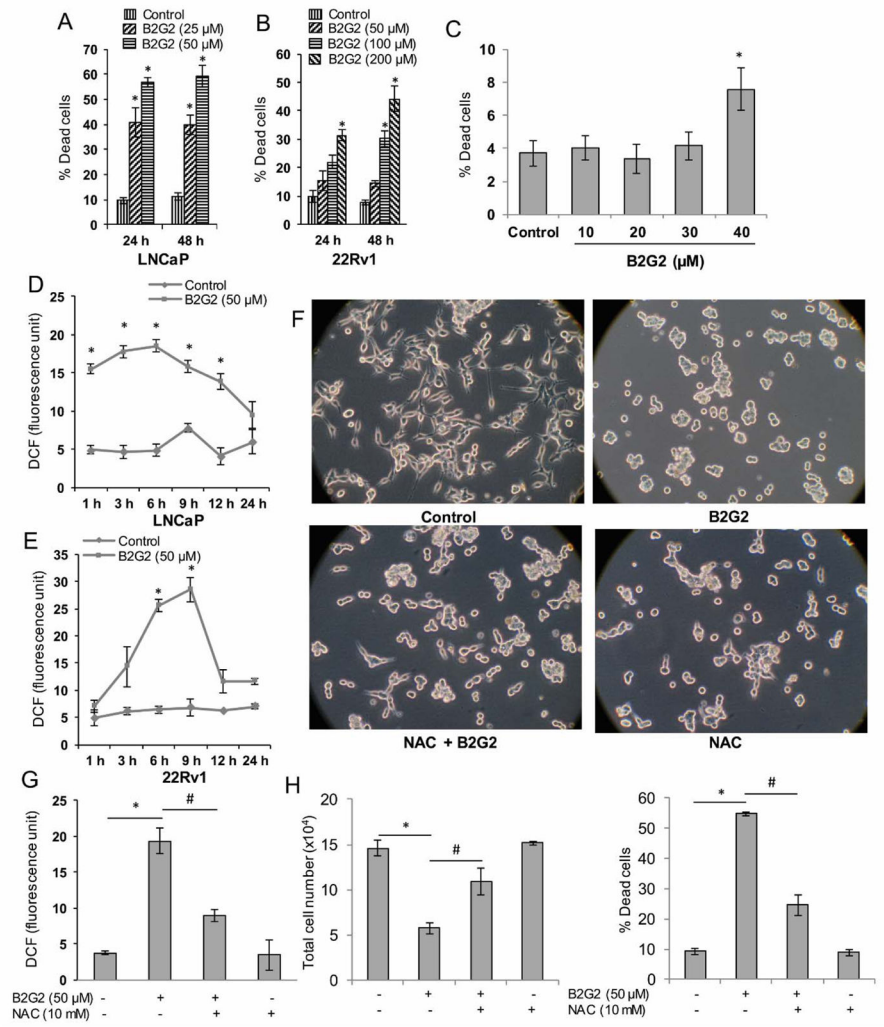

FIGURE 1. B2G2-induces cell death in human PCa cells via increasing ROS generation

A–B, LNCaP and 22Rv1 cells were treated with indicated doses of B2G2 for 24 and 48 h. At the end of each time point, floating and adherent cells were collected and dead cells percentage was measured. *C,* PWR-1E cells were treated with indicated doses of B2G2 for 24 h, and floating and adherent cells were collected and dead cells percentage was measured. *D–E,* LNCaP and 22Rv1 cells were treated with B2G2 (50 μM) for the indicated time points. At the end of each time point, ROS generation in terms of DCF (arbitrary fluorescence unit) was measured as described in the 'Materials and Methods' section. *E–G,* LNCaP cells were treated with NAC (10 mM) 15 min prior to B2G2 (50 μM) treatment and images were captured at the end of the experiment (24 h) and representative photographs are shown (*F*). In this experiment, ROS generation was measured at 6 h (*G*) and total cell number and percentage of cell death were determined via trypan blue assay at 24 h (*H*). In each case, data is expressed as mean ± SEM (n=3). * $P < 0.05$, significant with respect to control group; # $P < 0.05$, significant with respect to the B2G2-treated group.

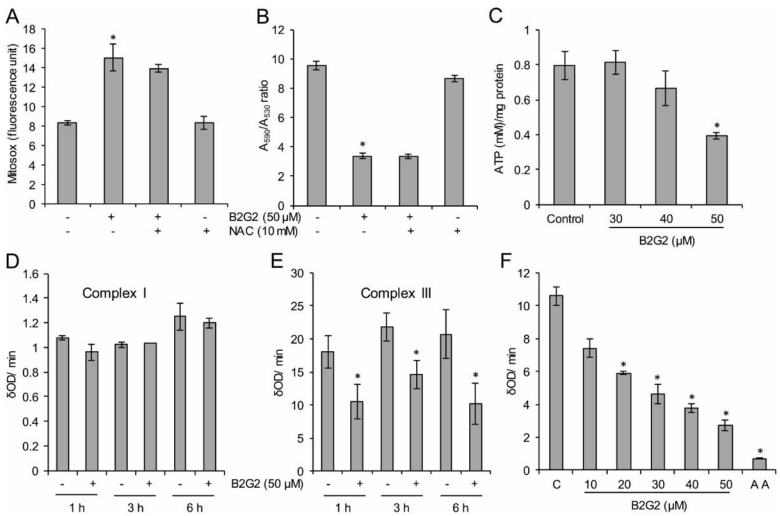

FIGURE 2. Effect of B2G2 on mitochondrial superoxide generation, mitochondrial membrane potential, ATP levels and activities of mitochondrial complexes I and III

A–B, LNCaP cells were treated with B2G2 (50 μM) with or without NAC (10 mM) for 6 h and mitochondrial superoxide generation was measured using MitoSox red dye (*A*); and mitochondrial membrane potential was measured using JC-1 dye (*B*). *C,* LNCaP cells were treated with different doses of B2G2 (30, 40 and 50 μM) and ATP level was measured after 6 h using an ATP assay kit. *D–E,* LNCaP cells treated with B2G2 (50 μM), mitochondria isolated after 1, 3 and 6 h and analyzed for mitochondrial complexes I and III activity. *F,* Mitochondria were isolated from naïve LNCaP cells and incubated with different concentrations of B2G2 (10–50 μM) and mitochondrial complex III activity was measured. Mitochondria treated with 3 μM antimycin (AA) served as positive control in this experiment. In each case, data is expressed as mean ± SEM (n=3). * $P < 0.05$, significant with respect to control group.

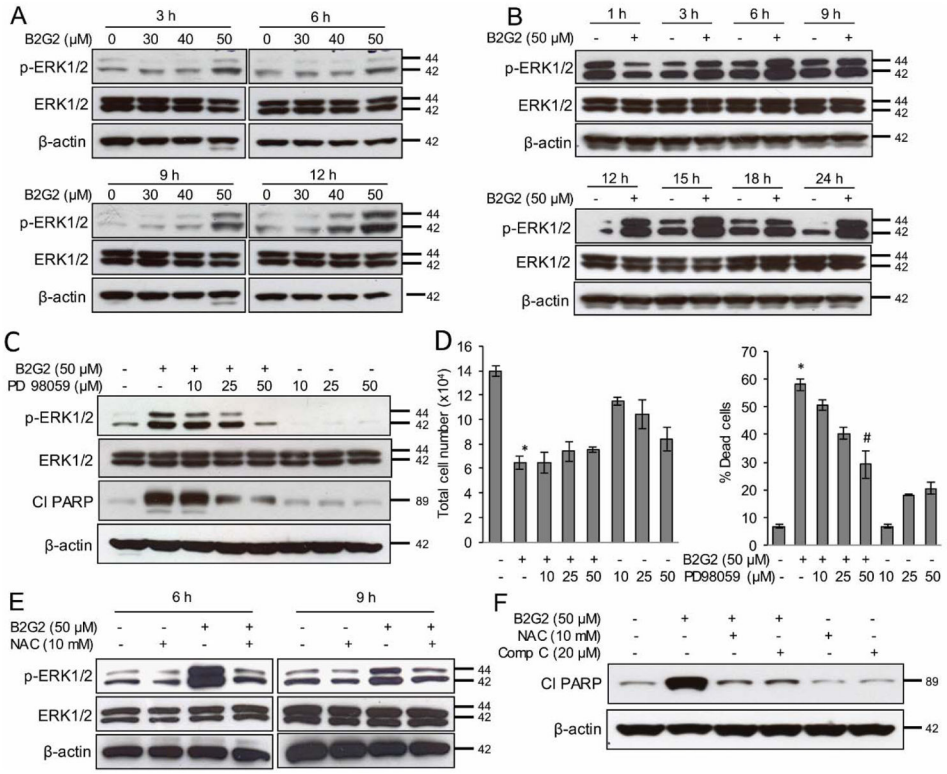

FIGURE 3. B2G2-induced cell death in PCA cells is through sustained ERK1/2 activation

A, LNCaP cells treated with different concentrations of B2G2 (30, 40 and 50 μM), whole cell lysates were prepared at indicated time-points and analyzed for p-ERK1/2 by immunoblotting. Membranes were stripped and re-probed for total ERK1/2 and β-actin. *B,* LNCaP cells were treated with B2G2 (50 μM), whole cell lysates were prepared at 1, 3, 6, 9, 12, 15, 18 and 24 h post-treatment and analyzed for p-ERK1/2 level by immunoblotting. Membranes were stripped and re-probed for total ERK1/2 and β-actin. *C–D,* LNCaP cells were treated with PD98059 (10, 25 and 50 μM) 15 min prior to B2G2 (50 μM) treatment and whole cell lysates were prepared at 24 h post-treatment and analyzed for p-ERK1/2 and cleaved PARP (cl PARP); membranes were stripped and re-probed for total ERK1/2 and β-actin (*C*); at the same time-point total cell number and percentage cell death were also determined by trypan blue exclusion assay (*D*). Data are expressed as of mean ± SEM (n=3) for each treatment. * $P < 0.05$, significant with respect to control group. # $P < 0.05$, significant with respect to the B2G2-treated group. *E,* LNCaP cells were treated with NAC (10 mM) 15 min prior to B2G2 (50 μM) treatment, whole cell lysates were prepared at 6 and 9 h post-treatment and analyzed for p-ERK1/2 by immunoblotting. Membranes were stripped and re-probed for total ERK1/2 and β-actin. *F,* LNCaP cells were treated with NAC (10 mM) or compound C (20 μM) prior to B2G2 (50 μM) treatment, whole cell lysates were prepared at 24 h and analyzed for cl PARP. Membrane was stripped and re-probed for β-actin.

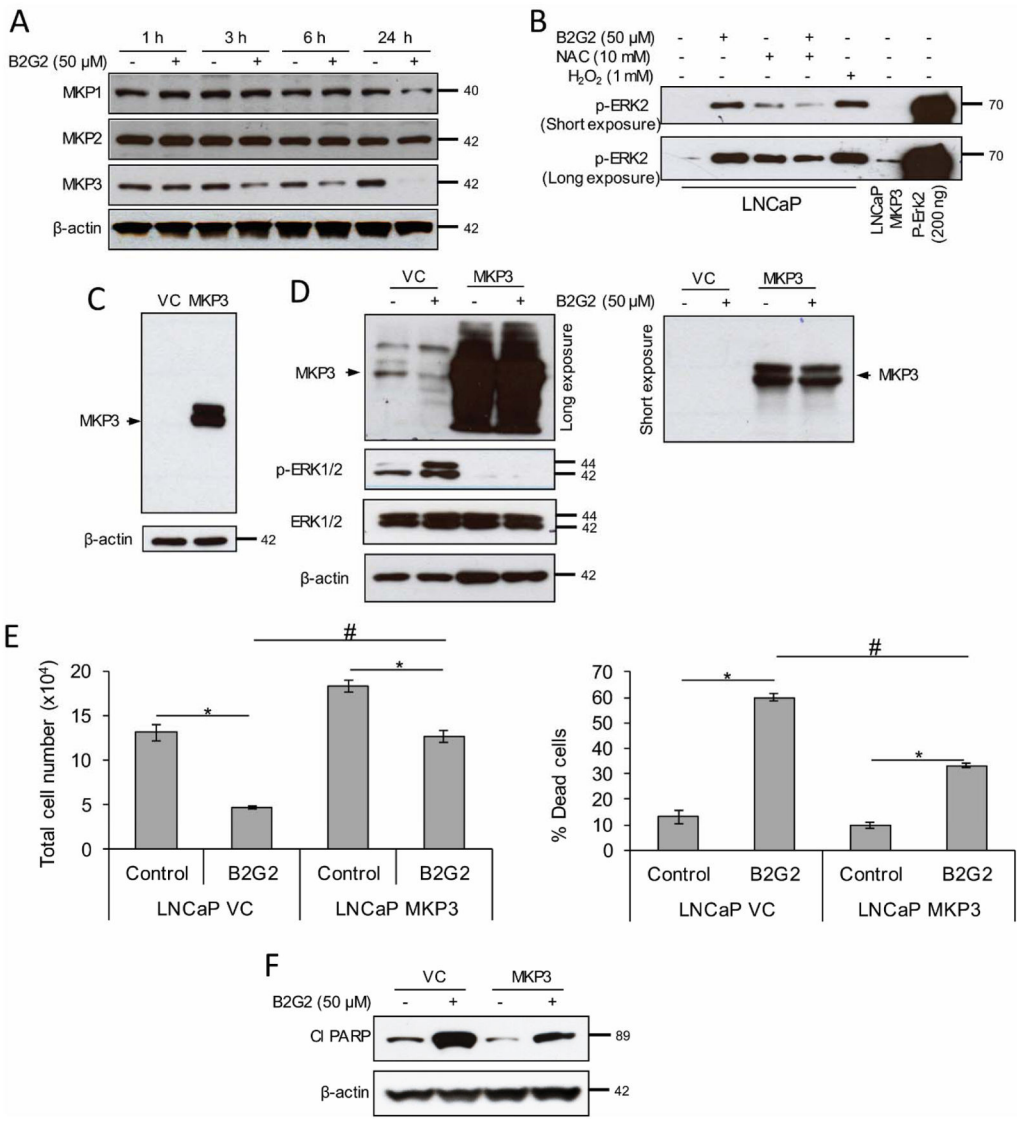

FIGURE 4. B2G2-induced death in LNCaP cells is through inhibiting MAP kinase phosphatase expression and activity

A, LNCaP cells were treated with B2G2 (50 μM), whole cell lysates were prepared at 1, 3, 6 and 24 h time points and analyzed for MKP1, MKP2 and MKP3 expression by immunoblotting. Membranes were stripped and re-probed for β-actin. *B,* LNCaP cells were treated with B2G2 (50 μM) with or without NAC (10 mM), protein lysates were prepared in phosphatase assay buffer at 6 h post-treatment and MAP kinase phosphatase activity was assessed using p-ERK2 as substrate as detailed in Materials and Methods' section. LNCaP cells treated with H_2O_2 (1.0 mM) served as negative control in this experiment, whereas, lysate prepared from MKP3-overexpressing LNCaP cells were used as positive control for this assay. Last lane was recombinant p-ERK2 protein. A short and long exposure of the blot is presented here. *C,* MKP3 expression in vector control and MKP3 overexpressing LNCaP cells was compared by immunoblotting. Membrane was stripped and re-probed for β-actin. *D,* LNCaP-VC and LNCaP-MKP3 cells were treated with B2G2 (50 μM), whole cell lysates

were prepared at 24 h time point and analyzed for MKP3 (long exposure-left panel; short exposure-upper right panel) and p-ERK1/2 (left panel) by immunoblotting. Membranes were stripped and re-probed for total ERK1/2 and β-actin (left panel). *E,* LNCaP-VC and LNCaP-MKP3 cells were treated with B2G2 (50 μM), total cell number and percentage cell death were determined by trypan blue exclusion assay at 24 h post-treatment. *F,* LNCaP-VC and LNCaP-MKP3 cells were treated with B2G2 (50 μM), whole cell lysates were prepared at 24 h time point and analyzed for cl PARP. Membrane was stripped and re-probed for β-actin. Data are expressed as of mean ± SEM (n=3) for each treatment. * $P < 0.05$, significant with respect to control group; # $P < 0.05$, significant with respect to B2G2-treated LNCaP-VC versus B2G2-treated LNCaP-MKP3 group.

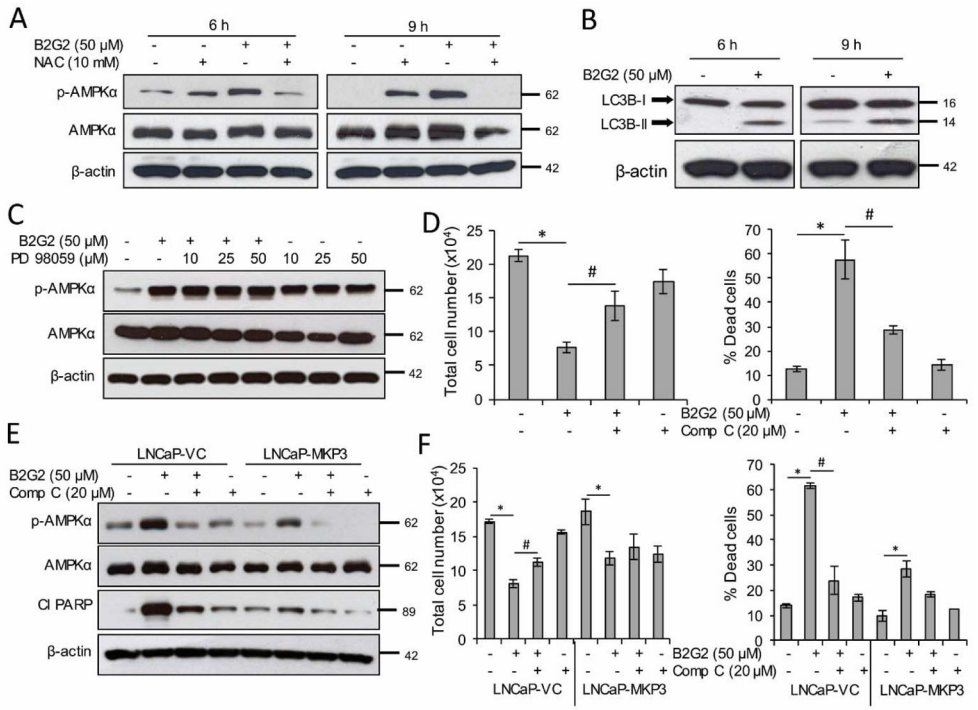

FIGURE 5. B2G2 activates AMPK through MKP3 inhibition and causes cell death in LNCaP cells

A, LNCaP cells were treated with NAC (10 mM) 15 min prior to B2G2 (50 μM) treatment, whole cell lysates were prepared at 6 and 9 h post-treatment and analyzed for p-AMPKα by immunoblotting. Membranes were stripped and re-probed for total AMPKα and β-actin. *B,* LNCaP cells were treated with B2G2 (50 μM), whole cell lysates were prepared at 6 and 9 h time points and analyzed for LC3B-I/II via immunoblotting. Membranes were stripped and re-probed for β-actin. *C,* LNCaP cells were treated with PD98059 (10, 25 and 50 μM) 15 min prior to B2G2 (50 μM) treatment, whole cell lysates were prepared at 24 h post-treatment and analyzed for p-AMPKα by immunoblotting. Membranes were stripped and re-probed for total AMPKα and β-actin. *D,* LNCaP cells were treated with compound C (20 μM) 15 min prior to B2G2 (50 μM) treatment and total cell number and percentage cell death were determined by trypan blue exclusion assay at the 24 h time point. Data are expressed as of mean ± SEM (n=3) for each treatment. * $P < 0.05$, significant with respect to control group; # $P < 0.05$, significant with respect to B2G2-treated group. *E,* LNCaP-VC and LNCaP-MKP3 cells were treated with compound C (20 μM) 15 min prior to B2G2 (50 μM) treatment, whole cell lysates were prepared after 24 h and analyzed for p-AMPKα and cleaved PARP by immunoblotting. Membranes were stripped and re-probed for total AMPKα and β-actin. *F,* In the same experiment, total cell number and percentage cell death were also determined via trypan blue exclusion assay after 24 h. Data are expressed as of mean ± SEM (n=3) for each treatment. * $P < 0.05$, significant with respect to control group; # $P < 0.05$, significant with respect to B2G2-treated group.

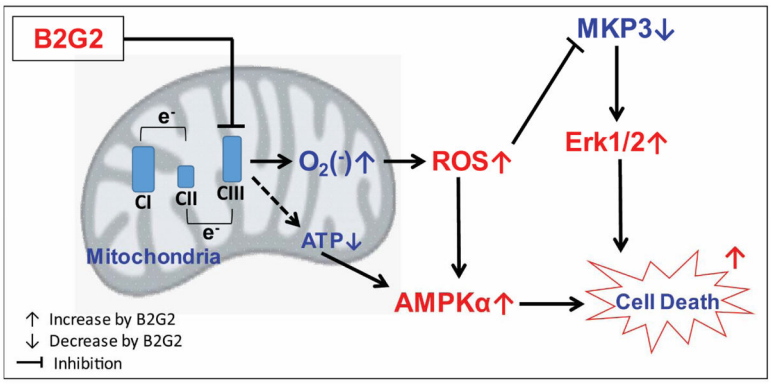

FIGURE 6. Schematic presentation of B2G2-induced death in human PCa cells

B2G2 treatment inhibits mitochondrial complex III activity leading to ROS generation, decrease in MKP3 activity and Erk1/2 activation. Further, B2G2 treatment decreases cellular ATP level resulting in AMPKα activation. Together, these molecular changes lead to death in human PCa cells by B2G2 treatment.